ORIGINAL ARTICLE

Development of a predictive model for preoperative bone metastasis risk assessment in prostate cancer through integration of semi-quantitative single-photon emission computed tomography/computed tomography indices with peripheral blood biomarkers

Pan Hao[1], Ruiqiang Xin[1], Yancui Li[1], Ran Guo[1], Lixin Sun[2], Yuanyuan Yang[2], Bingye Zhang[2], Min Jia[3]

[1]Medical Imaging Center, Beijing Luhe Hospital, Capital Medical University, Beijing, China, [2]Department of Nuclear Medicine, Beijing Luhe Hospital, Capital Medical University, Beijing, China, [3]Department of Urology, The Third Affiliated Hospital of Chongqing Medical University, Chongqing, China

Background: To investigate the risk factors of preoperative bone metastasis (BM) of prostate cancer (PCa) by using semi-quantitative single-photon emission computed tomography/computed tomography (SPECT/CT) whole-body bone imaging and peripheral blood biomarkers, and to establish a morphological map model to evaluate its prediction accuracy. **Materials and Methods:** Clinical data of 220 patients diagnosed with PCa were retrospectively analyzed. BM was identified using SPECT/CT. Based on the presence or absence of BM, patients were divided into two groups. Univariate and multiple logistic regression analyses were performed on various factors, including age, laboratory parameters, prostate volume determined, clinical tumor stage (cTx), and Gleason score (GS). Draw the receiver operating characteristic curve and calculate the area under the curve (AUC), and analyze the predictive efficacy. In addition, we construct a nomogram representing the BM prediction model using clinical data and generate a calibration plot to assess the accuracy of our predictions. **Results:** The analysis of univariate and multiple logistic regression demonstrated that (target area-nontarget area)/nontarget area (T-NT)/NT, alkaline phosphatase (ALP), total prostate-specific antigen (tPSA), cTx, and GS were independent predictors of BM in PCa. The tPSA displayed the highest AUC of 0.68 (95% confidence interval [CI]: 0.62–0.75) among the five independent predictors. The best predictive efficacy was shown when the predictive model was established using these five factors, as evidenced by the AUC of 0.80 (95% CI: 0.75–0.86) being higher than any single indicator. The predictive model's external validation data sensitivity and specificity metrics were 66.67% (8/12) and 95.65% (22/23), respectively, which were consistent with the model's initial sensitivity of 58.02% and specificity of 87.77%, indicating high accuracy and stability. **Conclusion:** The established predictive model, incorporating (T-NT)/NT from semi-quantitative SPECT/CT, ALP, tPSA, cTx, and GS, exhibits strong predictive efficacy with high accuracy and stability, providing a reliable tool for preoperative assessment of BM risk in PCa patients.

Key words: Biomarkers, bone metastasis, prediction model, prostate cancer, single-photon emission computed tomography/computed tomography

How to cite this article: Hao P, Xin R, Li Y, Guo R, Sun L, Yang Y, *et al.* Development of a predictive model for preoperative bone metastasis risk assessment in prostate cancer through integration of semi-quantitative single-photon emission computed tomography/computed tomography indices with peripheral blood biomarkers. J Res Med Sci 2025;30:64.

INTRODUCTION

Prostate cancer (PCa) is the second most common type of cancer in male, accounting for approximately 15% of all diagnosed cancers in men worldwide.[1] Metastasis is frequently observed in PCa, with bone metastasis (BM) being the most common site.[2,3] When patients with PCa acquire bone metastases, their quality of life and survival

Access this article online

Quick Response Code:

Website: https://journals.lww.com/jrms

DOI: 10.4103/jrms.jrms_325_24

Address for correspondence: Dr. Ruiqiang Xin, No. 82, Xinhuanan Road, Tongzhou, Beijing Luhe Hospital, Beijing 101149, China.
E-mail: rxin@ccmu.edu.cn

Submitted: 25-Jun-2024; **Revised:** 07-Oct-2025; **Accepted:** 04-Nov-2025; **Published:** 30-Dec-2025

rates decrease significantly. Hence, timely identification of systemic bone metastases in patients with PCa is crucial for establishing treatment plans and precisely evaluating prognosis.

Research has indicated that the occurrence of PCa is strongly linked to the age of an individual.[4] Recent research has also demonstrated a potential link between levels of inflammatory markers and malignant tumors.[5,6] Patients with malignant tumors may change their coagulation and fibrinolysis systems, leading to the identification of coagulation-fibrinolysis-related indicators as potential predictors of tumor prognosis.[7-9] Understanding the Gleason score (GS) is crucial in assessing the potential for tumor recurrence or metastasis in PCa.[10] Prostate-specific antigen (PSA) has been recognized for its diagnostic value in PCa.[11] Multiple studies have demonstrated a significant relationship between cTx and PCa BM.[12]

It has been established that PCa cells secrete endothelin-1 and various cytokines, stimulating osteoblast proliferation, promoting osteoclast generation, and bone resorption.[13] Therefore, the characteristic of PCa BM is osteoblastic. Thus, it is essential to analyze the risk factors for bone metastases in PCa using nuclear bone imaging to enhance the accuracy of diagnostic imaging and to enable individualized treatment options in a clinical setting.[14]

Currently, the utilization of semi-quantitative analysis in bone imaging is relatively infrequent in clinical practice due to constraints in imaging equipment and software technology.[15] There is limited research on the predictive significance of single-photon emission computed tomography/computed tomography (SPECT/CT) semi-quantitative parameters in combination with additional factors for predicting the metastasis of PCa to the bone. Conversely, this technology offers significant development opportunities and holds enormous potential for therapeutic applications. At the same time, international scholars have established many prediction models for BM of PCa, but most of them are based on MR, etc.[16] Due to regional and ethnic differences, the conclusions of these studies may not be applicable to the Chinese population. Based on this, the purpose of this study was to analyze and explore multiple possible predictors of PCa BM, such as SPECT/CT semi-quantitative indicators, age, laboratory parameters, prostate volume (PV), cTx, GS, and establish a nomogram. Finally, external data are used to verify the prediction model.

MATERIALS AND METHODS

Clinical data

Patient source

Our study was approved by the Ethics Committee of Luhe Hospital, Capital Medical University (no. 2024-LHKY-039-01). This study was retrospective and did not require patients to provide signed informed consent. This study retrospectively collected clinical data of newly diagnosed PCa patients at Luhe Hospital, Capital Medical University were selected from June 2022 to June 2023. Cases from July to September 2023 were used as external validation data. All the information included SPECT/CT semi-quantitative parameters, age, laboratory parameters (red blood cell count, serum calcium (Ca), hematocrit, hemoglobin, red cell distribution width coefficient of variation (CV), red cell distribution width standard deviation (SD), platelet count, platelet crit value, platelet distribution width, fibrinogen degradation products (FDP), absolute neutrophil count, neutrophil percentage, absolute lymphocyte count, lymphocyte percentage, absolute monocyte count, monocyte percentage, total PSA (tPSA), alkaline phosphatase (ALP), free PSA (fPSA), PV, cTx, and GS. According to the empirical method, 5–6 independent variables are expected to be included in the model. According to the expected present value (EPV) empirical method, if EPV is 10, the sample size is 50–60 cases per group. Case group: The control group was 1:1 to ensure sufficient sample size.

Inclusion criteria

Patients aged 18 or older who were diagnosed with PCa through transrectal prostate biopsy received whole-body bone planar imaging and local tomography. Two nuclear medicine experts with substantial expertise in this field verified their diagnosis. Patients with other complete clinical data required for this study were included.

Exclusion criteria

Patients with a history of other malignant tumors, urinary tract infections, or urinary retention, who had undergone invasive procedures like prostate biopsy within 3–5 days before PSA testing, had received biopsy pathology or treatment at other hospitals, were unable to confirm the presence of BM, or had missing data.

After excluding 26 people, the predictive model group consisted of 220 patients who met the inclusion criteria. In addition, an additional group of 35 patients meeting the same criteria was used for model validation.

Bone imaging

Bone imaging examination method

The imaging equipment used was the Siemens SymbiaT6 SPECT/CT system (Siemens, Germany), with 99mTc-methylene diphosphonate (99mTc-MDP) as the tracer. Each patient received an intravenous injection of 99mTc-MDP at a dose of 740–925 MBq (20–25 mCi). After tracer injection, patients were instructed to maintain adequate hydration (drinking 500–1000 mL of normal saline within 1 h postinjection) and empty their bladder

before imaging. The imaging acquisition was performed 3–4 h after tracer injection. A low-energy high-resolution collimator was used to optimize the spatial resolution of bone lesions while reducing scatter radiation. The SPECT acquisition matrix was set to 256 × 256, with a zoom factor of 1.0 (field of view covering the entire body from the skull to the proximal femurs). A 360° circular orbit acquisition was performed, with 64 projections per rotation and an acquisition time of 20–25 s per projection. After detecting anomalous concentrated lesions in whole-body bone imaging, SPECT/CT fusion imaging was conducted using the lesion as the focal site. If no significant abnormalities were found in the whole-body bone imaging, SPECT/CT fusion imaging was performed based on the location where the patient was experiencing the pain. Parameters are set to general parameters.[17]

Bone imaging diagnostic criteria

(1) Planar BM: Asymmetric foci of abnormal radioactive concentration were observed. The rib lesions manifested as either circular or elongated formations, while the spinal lesions were situated within the vertebral bodies and arches of the patient. BM was diagnosed based on an increased concentration or enlarged radioactive foci during re-examination, accompanied by severe or aggravated bone pain or the appearance of scattered radioactive foci in more than two locations.[18] (2) Planar no BM: No abnormal radioactive concentration foci were observed, or if present, they were located in surgical, fracture, or trauma sites. Rib lesions showed abnormal distribution perpendicular to the long axis of the rib. In suspected cases, follow-up imaging showed a decrease, disappearance, or no change in the concentration of the radioactive foci without any treatment. (3) Tomographic BM: CT imaging revealed abnormal radioactive distribution sites characterized by lytic and sclerotic bone destruction. These findings were not associated with surgery or fractures. Soft tissue mass shadows surrounding these locations were also identified.[19] (4) Tomographic no BM: The distribution area of abnormal radioactivity was consistent with surgical areas, nonpathological fracture areas, or benign bone lesions in CT images. Two experienced nuclear medicine physicians independently reviewed bone imaging diagnoses using a blind method. In the event of a difference in opinion, consensus was achieved through deliberation.

Setting of semi-quantitative parameters for bone imaging

On the local bone tomography images, regions displaying distinct lesion characteristics (e.g., abnormal radioactive concentration in vertebral bodies, ribs, or pelvic bones) or concentrated radioactive distribution were selected for semi-quantitative analysis. The region of interest (ROI) delineation protocol was standardized as follows: ROI selection criteria: For target area (T, lesion area), the ROI was manually delineated to fully cover the area of abnormal radioactive concentration, with a minimum pixel size of 10 × 10 pixels to avoid partial volume effects; for nontarget area (NT, normal bone tissue), the ROI was selected from the contralateral or adjacent normal bone tissue of the same anatomical site as T (e.g., if T was located in the right ilium, NT was selected from the left ilium), ensuring NT had no visible abnormal radioactive distribution and the same anatomical structure (e.g., cortical bone, cancellous bone) as T [Figure 1].[15] ROI operation specifications: All ROI delineations were performed using the built-in ROI tool of the Siemens SymbiaT6 SPECT/CT system (Version V10.0) by two independent nuclear medicine physicians (Physician A and Physician B, with 8 and 10 years of experience in nuclear bone imaging, respectively). Neither physician was aware of the patient's clinical diagnosis or BM status (blinded assessment). Repeatability test design: To assess intra-observer and inter-observer reproducibility of (T-NT)/NT, Physician A re-delineated the ROI of 30 randomly selected patients (15 with BM, 15 without BM) 2 weeks after the first delineation; Physician B delineated the same 30 patients' ROI independently. The (T-NT)/NT ratio was calculated for each delineation, and the intraclass correlation coefficient (ICC) was used to evaluate reproducibility.

- First line: A male patient, aged 72, with PCa BM. SPECT/CT transverse axis demonstrates intensified tracer uptake in the right ilium. Records count of the same T and NT areas, the (T-NT)/NT ratio was computed
- The second line: An 80-year-old male patient with nonbone metastatic PCa. SPECT/CT transverse axis shows increased tracer uptake at the five number vertebra. The area (T) counts the area (NT) counts and the (T-NT)/NT ratio was recorded.

Prostate volume calculation

Based on the color Doppler ultrasound, the dimensions of the prostate (left-right diameter, anterior–posterior diameter, superior–inferior diameter, in cm) were recorded. The PV was calculated using the formula: PV (cm^3) = Anterior–posterior diameter × Left–right diameter × Superior–inferior diameter × 0.52.

Gleason score evaluation criteria

The "Gleason classification system" was modified by the International Society of Urological Pathology in 2014.[20] And the modified GS was used in this study.

Clinical tumor stage

The clinical tumor stage (cTx) was classified according to the staging criteria provided by the American Joint Committee on Cancer in 2002.[21] In which "T1: A clinically occult tumor that cannot be palpated or detected by imaging," "T2: Tumor confined within the prostate gland," "T3: Tumor

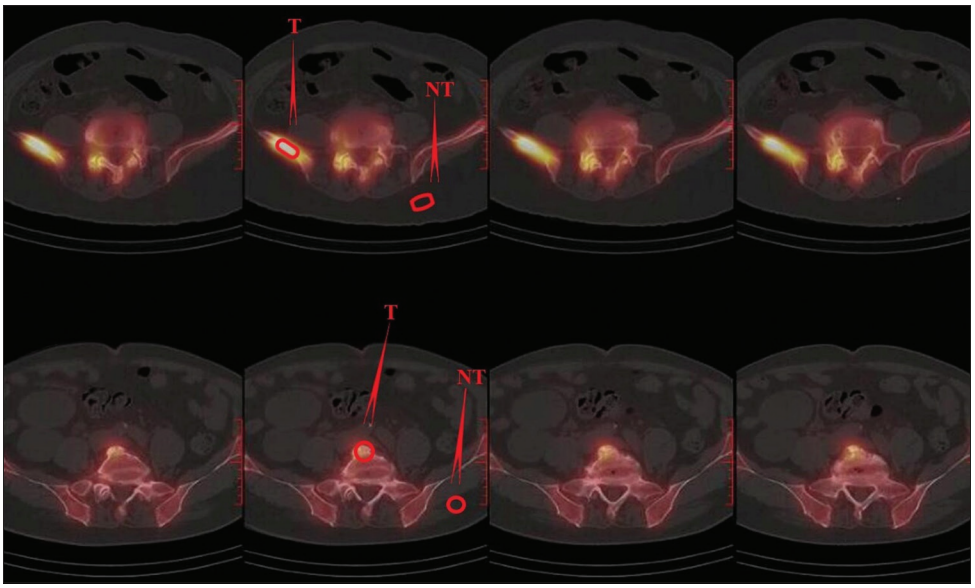

Figure 1: Parameters of bone metastasis/benign bone disease on tomography bone imaging

extending beyond the prostatic capsule (or tumor invading the seminal vesicles)," and "T4: Tumor is either fixed or has invaded the adjacent structures outside the prostate gland, such as the bladder neck, rectum, external urethral sphincter, legator ani muscle, or pelvic wall."

Laboratory parameters

PSA is detected using a chemiluminescent immunoassay analyzer and a corresponding immunoassay reagent kit. A fully automated biochemical analyzer measured other indicator levels.

Model external validation

Model external validation: The external validation data were substituted into the logistic regression of the prediction model, resulting in the probability distribution of BM and non-BM (NBM), as well as the sensitivity and specificity of the model. Compared with the results of the internal validation, these findings supported the accuracy and stability of the model.

Predictor selection strategy

To ensure the rationality and stability of the predictive factors, a three-dimensional selection strategy combining clinical significance, statistical testing, and model fitting efficiency was adopted, instead of relying solely on *P* values for prescreening.

Clinical significance-oriented initial screening

Candidate predictors were first selected based on existing evidence and biological plausibility for PCa BM. Specifically, (T-NT)/NT (semi-quantitative SPECT/CT index, reflecting abnormal radioactive uptake in bone lesions), tPSA (a classic marker for PCa progression), ALP (associated with osteoblastic activity in BM), cTx (indicating tumor invasion range), and GS (reflecting tumor malignancy) were included as initial candidates–all these factors have been reported to be closely related to PCa BM in previous studies, ensuring a reasonable association with the outcome variable (BM).

Statistical testing as a preliminary threshold

Univariate logistic regression analysis was performed to evaluate the association between each candidate predictor and BM. Variables with $P < 0.01$ were regarded as "potentially associated factors," while variables with no significant association (e.g., age, PV, serum calcium, $P > 0.05$) were excluded. Notably, the *P* value threshold was only used to eliminate variables with weak statistical relevance, not as the sole criterion for inclusion in the multivariable model.

Penalized regression for stability verification

To further validate the stability of the selected predictors and avoid overfitting, least absolute shrinkage and selection operator (LASSO) penalized regression was supplemented. The optimal λ value (penalty parameter) was determined via 10-fold cross-validation (minimum mean squared error criterion). The LASSO model was used to screen the initial candidate predictors, and the results were compared with the multivariable logistic regression model to confirm the consistency of the selected factors.

Statistical methods

The data analysis was conducted using the SPSS version 25.0 software. The one-sample Kolmogorov–Smirnov test was used to evaluate the normality of distribution for the continuous data. Normally distributed data were presented as mean ± SD ($\bar{x} \pm s$) and inter-group comparisons were analyzed using an independent sample *t*-test. Nonnormally distributed data were expressed as median and interquartile range, and the Mann–Whitney U test was applied for

group comparisons. For categorical data, they were summarized as frequencies or proportions. To compare categorical data between groups, the χ^2 test was utilized. To identify independent risk factors for BM in PCa, we first performed univariate logistic regression analyses to assess the association between each variable (including both categorical and continuous variables) and bone imaging results. Variables with statistical significance ($P < 0.01$) in the univariate analysis were then included in the multiple logistic regression model to further evaluate their independent associations with BM, after adjusting for potential confounding factors. Subsequently, the receiver operating characteristic (ROC) curve was generated based on the predicted probabilities from the logistic regression model, and the area under the curve (AUC) of the ROC was calculated. Finally, R 4.0 software (R Foundation for Statistical Computing, Vienna, Austria) was used to generate a nomogram (line diagram) to estimate the probability of BM in individual cases. Two-tailed $P < 0.05$ was considered statistically significant. To assess the internal validity of the predictive model, Bootstrap resampling (1000 repetitions) was used to calculate the optimism-corrected AUC and calibration parameters (slope and intercept).

RESULTS

Clinical and pathological characteristics

In this study, a total of 220 people were included in the BM group and the NBM group, and 26 people were excluded. In the model validation group, 35 people were included, and 2 were excluded.

Among the 81 cases in the BM group, the mean age was 72 (66.74) years, and the mean tPSA level was 284 (88.467) ng/mL. In the NBM group of 139 cases, the mean age was 72 (65.77) years, and the mean tPSA level was 52 (0.217) ng/mL. Among 220 PCa patients, GS, cTx, tPSA, fPSA, ALP, FDP, and (T-NT)/NT ratio were associated with the spread of cancer to the bones ($P < 0.05$) [Table 1].

Analysis of factors influencing bone metastasis

The reproducibility of the (T-NT)/NT ratio, evaluated by ICC based on 30 randomly selected patients, showed excellent consistency: Intra-observer reproducibility: The ICC of Physician A's two independent delineations was 0.94 (95% CI: 0.89–0.97, $P < 0.001$), indicating high consistency in (T-NT)/NT calculation by the same observer. Inter-observer reproducibility: The ICC between Physician A and Physician B's delineations was 0.92 (95% CI: 0.85–0.96, $P < 0.001$), confirming good consistency in (T-NT)/NT calculation between different observers.

The above results demonstrated that the (T-NT)/NT ratio had reliable reproducibility under the standardized ROI protocol, supporting its validity as a semi-quantitative indicator in the predictive model.

In the results, univariate logistic regression identified several factors associated with BM. Among these, only those with significant associations ($P < 0.01$) in the univariate analysis were included in the multivariable logistic regression. Multivariable logistic regression analysis revealed that GS, cTx, tPSA, ALP, and (T-NT)/NT ratio were identified as independent risk factors for BM in patients with PCa [$P < 0.01$, Table 2]. According to ROC curve analysis of individual variables, the value corresponding to the maximum Youden index was taken as the critical value. TPSA, cTx, and GS were converted into categorical variables with the best cutoff values: tPSA was divided into ≤236 ng/mL and >236 ng/mL; cTx was grouped into T1–T2 and T3–T4; GS was divided into ≤7 points and 8–10 points.

The receiver operating characteristic curve analysis and parametric characteristics for prostate cancer bone metastases

The ROC curve analysis revealed that the prediction model had the largest AUC [Figure 2]. The AUC was 0.804 (95% CI: 0.75–0.86), and the optimal diagnostic cutoff value for (T-NT)/NT was 5.3. This cutoff value corresponded to a sensitivity of 52.48% and a specificity of 76.46% for diagnosing BM. Moreover, the model exhibited higher specificity (87.77%, 95% CI: 82.1%–92.0%), with a positive predictive value (PPV) of 73.44% (95% CI: 65.3%–80.2%) and a negative predictive value (NPV) of 78.21% (95% CI: 71.5%-83.8%). The detailed diagnostic parameters of relevant indicators are summarized in Table 3.

Model internal validation

To reduce the optimism bias of the predictive model and verify its stability, we performed internal validation using the bootstrap resampling method (1000 repetitions) based

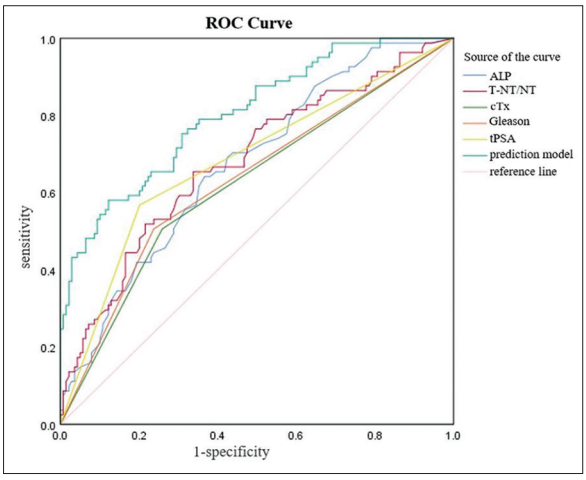

Figure 2: Assessment of receiver operating characteristic for risk factors and predictive models of bone metastases in prostate cancer

Table 1: Clinical basic data of patients with prostate cancer and comparison between groups

Variables	Total patients (*n*=220)	NBM (*n*=139)	BM (*n*=81)	*P*
tPSA (ng/mL)	103 (0–304)	52 (0–217)	283 (88–467)	0.000
ALP (U/L)	81.9±21.5	76.9±20.5	90.5±20.4	0.000
T-NT/NT	5.1±1.1	4.9±1.0	5.5±1.1	0.000
fPSA (ng/mL)	8.1 (6.0–10.7)	7.6 (4.8–10.2)	9.3 (6.5–11.9)	0.004
Prostatic volume (cm^3)	79.4 (55.5–102.7)	76.4 (54.7–113.6)	82.2 (56.3–100.7)	0.685
Age (years)	72 (65–76)	72 (65–77)	72 (66–74)	0.375
Ca (mmol/L)	2.2 (2.1–2.3)	2.2 (2.2–2.3)	2.2 (2.1–2.3)	0.395
RBC (10^{12}/L)	4.2 (3.7–4.6)	4.2 (3.7–4.6)	4.2 (3.7–4.6)	0.519
FDP (g/L)	3.3 (2.8–4.3)	3.1 (2.7–3.9)	3.8 (3.1–4.5)	0.000
Absolute neutrophil count (10^9/L)	3.3 (2.3–4.7)	3.4 (2.4–4.7)	3.3 (2.3–4.7)	0.761
Lymphocyte count (10^9/L)	1.5 (1.1–1.8)	1.5 (1.1–1.8)	1.5 (1.2–1.9)	0.882
Absolute monocyte count (10^9/L)	0.5 (0.4–0.6)	0.5 (0.4–0.6)	0.5 (0.3–0.6)	0.854
Monocyte percentage (%)	8.2 (7.1–10.1)	8.1 (7.1–10.1)	8.2 (7.1–10.2)	0.736
Neutrophil percentage (%)	61.2±9.7	61.1±9.8	61.4±9.6	0.776
Lymphocyte percentage (%)	27.0 (18.4–32.1)	27.5 (18.7–32.1)	25.9 (16.7–32.2)	0.400
Hb (g/L)	135.0 (111.8–146.0)	135.0 (117.0–146.0)	133.0 (109.0–145.5)	0.170
Hematocrit (L/L)	0.41 (0.35–0.44)	0.41 (0.35–0.44)	0.40 (0.32–0.43)	0.216
Red cell distribution width CV (%)	13.4 (12.8–14.0)	13.3 (12.6–13.9)	13.6 (12.9–14.9)	0.099
Red cell distribution width SD (fL)	44.4 (42.4–47.2)	43.8 (42.3–46.7)	44.6 (42.4–47.3)	0.215
PLT (10^9/L)	191.0 (163.0–216.0)	191.0 (157.0–216.0)	195.0 (169.5–215.0)	0.236
Platelet crit value (L/L)	0.2 (0.1–0.2)	0.2 (0.1–0.2)	0.2 (0.1–0.2)	0.582
Platelet distribution width (fL)	16.7 (16.4–17.1)	16.7 (16.4–17.2)	16.7 (16.4–17.1)	0.654
Gleason, *n* (%)				
≤6	67 (30.45)	51 (36.69)	16 (19.75)	0.000
7	79 (35.91)	55 (39.57)	24 (29.63)	
8	53 (24.09)	25 (17.99)	28 (34.57)	
9	17 (7.73)	7 (5.04)	10 (12.35)	
10	4 (1.82)	1 (0.72)	3 (3.70)	
cTx, *n* (%)				
T1	49 (22.27)	41 (29.50)	8 (9.88)	0.000
T2	94 (42.73)	62 (44.60)	32 (39.51)	
T3	65 (29.55)	33 (23.74)	32 (39.51)	
T4	12 (5.45)	3 (2.16)	9 (11.11)	

Categorical variables are presented as numbers with percentages in parentheses, and continuous variables are shown as medians with interquartile in parentheses. ALP=Alkaline phosphatase; BM=Bone metastasis; cTx=Clinical tumor stage; Ca=Serum calcium; fPSA=Free prostate specific antigen; FDP=Fibrinogen degradation products; Hb=Hemoglobin; NBM=Non-bone metastasis; PLT=Platelet count; RBC=Red blood cell count; tPSA=Total prostate-specific antigen; T-NT/NT=Target area - nontarget area/ nontarget area; CV=Coefficient of variation; SD=Standard deviation; tPSA=Total prostate-specific antigen

Table 2: The risk factors, multiple logistic regression logistic analysis of bone metastasis (*n*=220)

	B	SE	Wald	DF	*P*	OR	OR 95% CI	
							Lower bound	Upper bound
ALP	0.036	0.008	9.588	1	0.002	1.026	1.010	1.044
T-NT/NT	0.439	0.172	6.504	1	0.011	1.551	1.107	2.174
cTx layering	0.974	0.346	7.908	1	0.005	2.648	1.343	5.219
Gleason layering	0.897	0.352	6.497	1	0.011	2.452	1.230	4.887
tPSA layering	1.217	0.346	12.389	1	0.000	3.378	1.715	6.653
Constant	−6.135	1.178	27.141	1	0.000	0.002		

All data in parentheses are 95% CI. CI=Confidential intervals; *B*=Regression coefficient; DF=Degree of freedom; OR=Odds ratio; SE=Standard error; WS=Wald statistic; ALP=Alkaline phosphatase; tPSA=Total prostate-specific antigen; cTx=Clinical tumor stage

on the original training set (220 PCa patients). The validation procedure was as follows: In each repetition, a sample of the same size as the original set was drawn with replacement from the 220 patients; a new logistic predictive model was reconstructed using the resampled dataset, and the performance metrics of the new model were recorded. After 1000 repetitions, the optimism value and validated metrics were calculated by comparing the performance differences between the models built on resampled datasets and the original model.

The results showed that:

- AUC after optimism correction: The AUC of the original

Table 3: Parametric characteristics of receiver operating characteristic for prostate cancer bone metastasis prediction

Variable	AUC (95% CI)	SE	Sensitivity	Specificity	PPV	NPV
ALP	0.675 (0.60–0.75)	0.037	64.2	63.31	50.49	75.21
T-NT/NT	0.681 (0.61–0.76)	0.038	65.43	66.19	52.48	76.47
cTx layering	0.624 (0.56–0.69)	0.034	50.62	74.1	53.25	72.03
Gleason layering	0.634 (0.60–0.70)	0.033	50.62	76.26	55.41	72.6
tPSA layering	0.683 (0.62–0.75)	0.033	56.79	79.86	62.16	76.03
Prediction model	0.804 (0.75–0.86)	0.03	58.02	87.77	73.44	78.21

All data in parentheses are 95% CI. The C-index (concordance index) of the prediction model is equivalent to the AUC; which is 0.804 (95% CI=0.75–0.86). Units of variables are as follows=ALP (U/L); tPSA (ng/mL); (T-NT)/NT (dimensionless); cTx and GS are categorical/score variables with no unit. The cutoff value of tPSA (236 ng/mL) is rounded from the original 235.507 ng/mL for clinical practicability. AUC=Area under the receiver operating characteristic curve; NPV=negative predictive value; PPV=Positive predictive value; ROC=Receiver operating characteristic; SE=Standard error; CI=Confidence intervals; ALP=Alkaline phosphatase; tPSA=Total prostate-specific antigen; cTx=Clinical tumor stage; T-NT/NT=Target area-nontarget area/nontarget area; GS=Gleason score

model in the training set was 0.804 [95% CI: 0.75–0.86, consistent with Table 3]. The optimism value (optimism) calculated by bootstrap validation was 0.032, and the AUC after correction was 0.772 (95% CI: 0.71–0.83), indicating that the model still maintained good discriminative ability after excluding optimism bias

- Calibration parameters after optimism correction: The corrected calibration slope was 0.99 (95% CI: 0.88–1.10), and the corrected intercept was −0.02 (95% CI: −0.18 to 0.14). The corrected slope was close to 1, and the intercept was close to 0, which suggested that the consistency between the predicted probability of BM and the actual risk was further improved, and the calibration performance of the model was stable and reliable.

Nomogram of prediction model

The prediction model of the nomogram, as shown in Figure 3, and its consistency index (C-index) is 0.804, indicating that the prediction accuracy of the model is high. Input indicators include T-NT/NT, GS, cTx, tPSA, and ALP. The output indexes included the input index scale, total score scale, and positive prediction probability of BM.

The calibration curve of the prediction model

The calibration curve (e calibration curve) of the prediction model is shown in Figure 4, with the X-axis representing nomogram prediction probability, Y-axis representing the actual probability, average absolute error = 0.0039, the apparent prediction model is the predicted value distribution curve, bias-corrected is the distribution curve after calibration bias, and ideal is the ideal curve. The curve of the prediction model overlaps with the calibration curve, and is biased from the ideal curve.

Model external validation

External validation data were applied to the nomogram of the predictive modeling framework to obtain the distribution of predicted probabilities [Table 4], which shows that NBM patients (without actual BM) predominantly cluster in low-probability intervals (4 cases in <0.1, 8 in 0.1–0.2) with 11 in medium-high intervals (0.2–0.7) indicating potential false positives, while BM patients (with actual BM) concentrate in medium-high intervals (none in <0.3, 12 scattered across 0.3–0.9+), showing the model identifies medium-high risks but with limited precision, with the model having reliable basic recognition for nonmetastasis and low risk of missed metastasis yet false positive risks and insufficient prediction accuracy for metastasis requiring further optimization; in the validation data, all 16 patients with a predicted probability of BM <0.3 were BM-negative, all 5 patients with a predicted probability ≥0.7 were BM-positive, and the external validation showed the model had a sensitivity (SEN) of 66.67% (8/12, 95% CI: 38.4%–88.2%) and a specificity (SPE) of 95.65% (22/23, 95% CI: 78.2%–99.9%). In addition, the PPV of the external validation model was 90.91% (95% CI: 58.7%–99.8%), and the NPV was 84.62% (95% CI: 65.1%–95.6%), further confirming the model's reliability in external cohorts.

DISCUSSION

PCa tends to first metastasize to the bones rather than other visceral organs.[22] Identifying the significant risk factors contributing to BM in patients with PCa is crucial for promoting early detection and tailored treatment approaches in clinical settings. CT and magnetic resonance imaging (MRI) exhibit high sensitivity and specificity for diagnosing systemic BM in PCa.[23,24] However, they cannot perform a comprehensive systemic assessment. Radionuclide whole-body bone scintigraphy is the primary diagnostic technique used in clinical practice to detect and monitor the presence of malignant tumor bone metastases.

Scintigraphy of the entire body's bones is based on the exchange and chemical adsorption of imaging agent 99Tcm-MDP with hydroxyapatite crystals in bones. Metastatic lesions show significant sensitivity in the imaging agent deposition, manifesting as aberrant imaging agent accumulation. SPECT/CT multimodal fusion bone scintigraphy offers benefits in terms of improved diagnostic accuracy. By exploiting the higher spatial resolution of CT scans, it can accurately locate anatomical structures and distinguish between benign and malignant pathologies. Compared to solely whole-body planar bone scintigraphy,

Table 4: Predicted probability distribution of bone metastasis and nonbone metastasis populations based on the predictive model

P	<0.1	0.1–0.2	0.2–0.3	0.3–0.4	0.4–0.5	0.5–0.6	0.6–0.7	0.7–0.8	0.8–0.9	≥0.9	Total
NBM	4	8	4	4	2	0	1	0	0	0	23
BM	0	0	0	2	2	3	0	3	1	1	12

The model sensitivity was 66.67% (8/12) with a Wilson binomial 95% CI of 38.4%–88.2%; the specificity was 95.65% (22/23) with a Wilson binomial 95% CI of 78.99%–99.25%. BM=Bone metastasis; NBM=Nonbone metastasis; *P*=Means probability; CI=Confidence interval

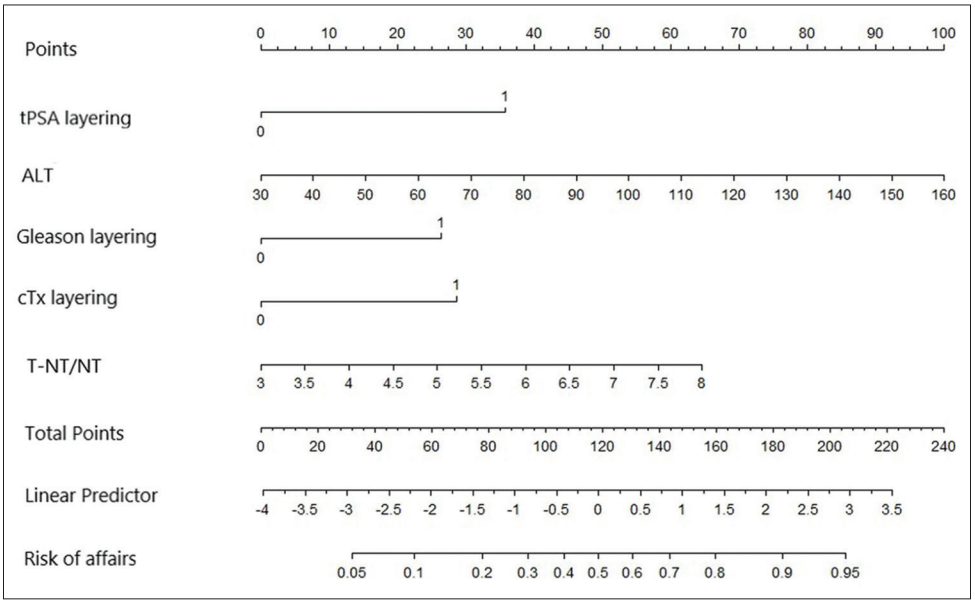

Figure 3: Nomogram of prediction model

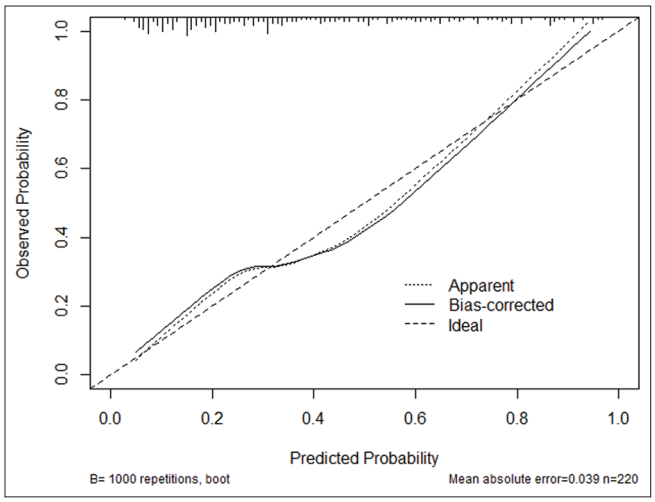

Figure 4: Calibration curve of the nomogram prediction model

it demonstrates better diagnostic accuracy and higher sensitivity in BM, receiving clear clinical affirmation.

In this study, semi-quantitative analysis parameters of local sectional bone scintigraphy were introduced, utilizing the (T-NT)/NT ratio to reflect the degree of abnormal radiotracer accumulation quantitatively. Setting semi-quantitative parameters of bone scintigraphy on local sectional CT fusion images can effectively avoid the issue of tissue overlap in planar imaging, facilitating delineation of the ROI for both diseased and normal bone tissues, with the detection of radioactive activity within these regions as well.[25] In the current study, it was found that the (T-NT)/NT ratio in the group with bone metastases was 5.5 ± 1.1, significantly higher than that in the NBM group, 4.9 ± 1.0 ($P < 0.01$), consistent with relevant reports.[18] The ROC analysis in this study showed that the critical value of (T-NT)/NT was 5.3. When it was >5.3, the diagnosis of BM was optimal, with a specificity and sensitivity for diagnosing BM of 66.19% and 65.43%, respectively.

Studies suggest that age is a risk factor for the development of PCa with BM.[26] Chaoying *et al*.[27] analyzed clinical data from 235 patients with PCa, and the results showed that age is one of the risk factors for PCa BM, with the incidence increasing with age. However, data from this study show no statistically significant age difference between the PCa BM and NBM groups ($P = 0.375$), consistent with another study.[28] This could be due to the relatively small sample size included in the study.

PSA is an essential indicator used to diagnose and differentiate PCa. Numerous studies have also indicated its value in diagnosing PCa BM.[29] The tPSA levels in this study showed a statistically significant difference ($P < 0.01$)

between the BM and NBM groups, with the BM group having significantly higher levels (284[88.467]) than the NBM group (52 [0.217]). The ROC curve analysis in this study revealed a critical for tPSA, with a sensitivity and specificity of 56.79% and 79.86%, respectively, in diagnosing PCa BM. Elevated PSA levels and the established cutoff value can be used to preliminarily screen suspected patients with BM, providing a reliable reference for the final diagnosis of BM.

The Gleason grading system is a standard pathological grading system for PCa, originating from the PCa growth pattern chart drawn by Gleason in 1966. Higher scores indicate a lower degree of differentiation and poorer prognosis. This approach is widely employed in clinical settings to evaluate the malignancy of PCa.[30] This study showed a statistically significant difference in GS scores between the BM group and the NBM group ($P < 0.01$).

ALP belongs to the phosphatase class of hydrolases, acting on the phosphate groups of free phosphate esters. Osteoblasts mainly secrete it and have long been considered a marker of osteoblast activity, which is an early biochemical indicator for detecting BM in PCa.[31] As reported previously,[32] BM is likely in PCa patients experiencing bone pain with serum ALP levels >90 U/L. This study showed a significant intergroup difference in ALP levels between the BM and NBM groups ($P < 0.001$), and the statistical analysis results confirmed ALP as an independent risk factor. It was determined that ALP = 82.5 U/L was the optimal diagnostic threshold in this study. ALP exhibited the lowest specificity among all independent risk factors at 63.31%, with a sensitivity of 64.2% and an AUC of 0.675. This may be due to the fact that bone chemokines can be used as chemokines of circulating prostate tumor cells. Once they reach the bone, they will be exposed to the bone microenvironment that supports metastatic growth. Then, the growth factors produced by tumor cells can directly stimulate the activity of osteoblasts, resulting in increased expression of RANK ligand, thus forming a vicious cycle. As a result, the level of ALP in the serum increases.[33]

Internationally, there are several tumor staging systems for PCa BM, with TNM staging being the most common. Later T staging indicates a wider tumor invasion and poorer prognosis. Multiple studies have shown a significant relationship between cTx and PCa BM.[34] There is a consensus that the risk of BM increases significantly when PCa reaches the T4 stage. This study revealed a statistically significant difference in cTx between the BM and NBM groups. Analysis showed that cTx = T3 was the optimal threshold, with a high level of sensitivity (50.62%), specificity (74.1%), and an AUC of 0.624.

In addition to the aforementioned predictive factors, BM risk factors may include inflammatory and coagulation markers[35,36] and serum calcium level. It is well known that the bone microenvironment provides a favorable environment for tumor cell growth and aggressiveness.[37] In recent years, a number of studies have shown that the occurrence and development of malignant tumors are closely related to the interaction between tumor characteristics and the body's inflammatory response, and tumor cell infiltration leads to tissue destruction, and then causes the body's nonspecific inflammatory response.[36] Some studies[38] have shown that tumor cell activation of the coagulation and fibrinolysis systems contributes to invasion and metastasis. However, there is no consistent conclusion between domestic and foreign researches. In this study, ALP was a risk factor for BM, while there was no significant difference in other relevant indicators.

In summary, when (T-NT)/NT > 5.3, the diagnostic efficiency for lesions is optimal, providing certain guidance for diagnosing BM in PCa. The tPSA emerges as a primary independent risk factor for diagnosing PCa BM, especially when tPSA > 236 ng/mL, indicating significant diagnostic importance for BM. TPSA had the highest AUC of 0.683. This suggests that tPSA has the optimal predictive performance for PCa BM. There is an increased probability of BM occurring in newly diagnosed PCa patients with a higher GS. There is a significant difference in cTx between the BM and NBM groups, and cTx is an independent predictor that can predict the development of BM in PCa. Moreover, there is a positive association between elevated levels of ALP in recently diagnosed PCa patients and a higher probability of BM, indicating that ALP might serve as a good predictor for BM in these individuals. When establishing a prediction model using all five factors, the AUC was 0.804 (95%CI: 0.75–0.86), greater than any single indicator. Moreover, the model displayed higher specificity (87.77%), with a PPV of 73.44% and an NPV of 78.21%, demonstrating the best predictive efficiency. Using these data, a nomogram can accurately predict the risk of BM. These nomograms may be used in clinical practice to provide personalized diagnosis and therapy. Furthermore, the C-index was calculated to indicate predictive accuracy, equivalent to the AUC, and ranged from 0.5 to 1.0. In this study, the C-index was 0.804, indicating the high accuracy of the predictive model. Finally, validation with 35 external data sets demonstrated the high accuracy and stability of the model, making it suitable for application in other datasets. The acquired results during model establishment, with a sensitivity of 58.02% and specificity of 87.77%, were consistent. This indicates that the model has an acceptable level of accuracy and stability.

CONCLUSION

However, this study has certain limitations. First, the specificity of SPECT/CT for diagnosing BM is slightly

inadequate. If conditions permit, using prostate-specific membrane antigen-positron emission tomography/CT or MRI for diagnosing BM may yield better results. Second, many factors can interfere with the selection and delineation of ROI in (T-NT)/NT measurements. Third, this study is retrospective with a limited number of cases included. The establishment of the model requires a large sample size to encompass a more comprehensive dataset, thus improving the accuracy of the predictive model.

Acknowledgments

The authors would like to thank my colleagues in the Nuclear Medicine department and the Department of Medical Imaging, Beijing Luhe Hospital, affiliated with Capital Medical University, and the Department of Urology, The Third Affiliated Hospital of Chongqing Medical University, Chongqing. The generous provision of a substantial number of patient pathology results has been invaluable to the research. Their expertise and skills have served as a crucial source of data and information for the study. The achievements of this research would not have been possible without their hard work and contributions.

Financial support and sponsorship

This work was supported by the 2020 Annual Science and Technology Plan Project of Tongzhou District, Beijing (Project Number: KJ2020CX004-03) and the National Natural Science Foundation of Chongqing (Project Number: cstc2021jcyj-msxmX0117).

Conflicts of interest

There are no conflicts of interest.

REFERENCES

1. Sung H, Ferlay J, Siegel RL, Laversanne M, Soerjomataram I, Jemal A, *et al*. Global cancer statistics 2020: GLOBOCAN estimates of incidence and mortality worldwide for 36 cancers in 185 countries. CA Cancer J Clin 2021;71:209-49.
2. Rodrigues DN, Butler LM, Estelles DL, de Bono JS. Molecular pathology and prostate cancer therapeutics: From biology to bedside. J Pathol 2014;232:178-84.
3. Ali A, Hoyle A, Haran ÁM, Brawley CD, Cook A, Amos C, *et al*. Association of bone metastatic burden with survival benefit from prostate radiotherapy in patients with newly diagnosed metastatic prostate cancer: A secondary analysis of a randomized clinical trial. JAMA Oncol 2021;7:555-63.
4. Sheikhbahaei S, Jones KM, Werner RA, Salas-Fragomeni RA, Marcus CV, Higuchi T, *et al*. (18)F-NaF-PET/CT for the detection of bone metastasis in prostate cancer: A meta-analysis of diagnostic accuracy studies. Ann Nucl Med 2019;33:351-61.
5. Cheng L, Li Z, Zheng Q, Yao Q. Correlation study of serum lipid levels and lipid metabolism-related genes in cervical cancer. Front Oncol 2024;14:1384778.
6. Li Y, Xu T, Wang X, Jia X, Ren M, Wang X. The prognostic utility of preoperative neutrophil-to-lymphocyte ratio (NLR) in patients with colorectal liver metastasis: A systematic review and meta-analysis. Cancer Cell Int 2023;23:39.
7. Tqian R, Yan H, Zhang F. Cumulative score based on preoperative plasma fibrinogen and serum C-reactive protein could predict long-term survival for esophageal squamous cell carcinoma. Oncotarget 2016;7:61533-43.
8. Chien TM, Lu YM, Geng JH, Huang TY, Ke HL, Huang CN, *et al*. Predictors of positive bone metastasis in newly diagnosed prostate cancer patients. Asian Pac J Cancer Prev 2016;17:1187-91.
9. McArthur C, McLaughlin G, Meddings RN. Changing the referral criteria for bone scan in newly diagnosed prostate cancer patients. Br J Radiol 2012;85:390-4.
10. Klaassen Z, Howard LE, de Hoedt A, Amling CL, Aronson WJ, Cooperberg MR, *et al*. Factors predicting skeletal-related events in patients with bone metastatic castration-resistant prostate cancer. Cancer 2017;123:1528-35.
11. Owari T, Miyake M, Nakai Y, Morizawa Y, Itami Y, Hori S, *et al*. Clinical features and risk factors of skeletal-related events in genitourinary cancer patients with bone metastasis: A retrospective analysis of prostate cancer, renal cell carcinoma, and urothelial carcinoma. Oncology 2018;95:170-8.
12. Coleman RE. Clinical features of metastatic bone disease and risk of skeletal morbidity. Clin Cancer Res 2006;12:6243s-9s.
13. Fizazi K, Carducci M, Smith M, Damião R, Brown J, Karsh L, *et al*. Denosumab versus zoledronic acid for treatment of bone metastases in men with castration-resistant prostate cancer: A randomised, double-blind study. Lancet 2011;377:813-22.
14. Lin Y, Mao Q, Chen B, Wang L, Liu B, Zheng X, *et al*. When to perform bone scintigraphy in patients with newly diagnosed prostate cancer? A retrospective study. BMC Urol 2017;17:41.
15. Yamane T, Fukushima K, Shirotake S, Nishimoto K, Okabe T, Oyama M, *et al*. Test-retest repeatability of quantitative bone SPECT/CT. Ann Nucl Med 2021;35:338-46.
16. Liu WC, Li MX, Qian WX, Luo ZW, Liao WJ, Liu ZL, *et al*. Application of machine learning techniques to predict bone metastasis in patients with prostate cancer. Cancer Manag Res 2021;13:8723-36.
17. Alqahtani MM, Fulton R, Constable C, Willowson KP, Kench PL. Diagnostic performance of whole-body SPECT/CT in bone metastasis detection using (99m) Tc-labelled diphosphate: A systematic review and meta-analysis. Clin Radiol 2020;75:961.e11-24.
18. Abikhzer G, Srour S, Fried G, Drumea K, Kozlener E, Frenkel A, *et al*. Prospective comparison of whole-body bone SPECT and sodium 18F-fluoride PET in the detection of bone metastases from breast cancer. Nucl Med Commun 2016;37:1160-8.
19. Cook GJ, Azad G, Padhani AR. Bone imaging in prostate cancer: The evolving roles of nuclear medicine and radiology. Clin Transl Imaging 2016;4:439-47.
20. Epstein JI, Egevad L, Amin WB .The 2014 International Society of Urological Pathology (ISUP) Consensus Conference on Gleason Grading of Prostatic Carcinoma: Definition of Grading Patterns and Proposal for a New Grading System.Am J Surg Pathol 2016;40:244-52.
21. Dash A, Sanda MG, Yu M. Prostate cancer involving the bladder neck. Urology 2002;60:276-80.
22. Moslehi M, Cheki M, Salehi-Marzijarani M, Amuchastegui T, Gholamrezanezhad A. Predictors of bone metastasis in pre-treatment staging of asymptomatic treatment-naïve patients with prostate cancer. Rev Esp Med Nucl Imagen Mol 2013;32:286-9.
23. Yu F, Yang M, He C, Yang Y, Peng Y, Yang H, *et al*. CT radiomics combined with clinical and radiological factors predict hematoma expansion in hypertensive intracerebral hemorrhage. Eur Radiol 2025;35:6-19.
24. De Visschere PJ, Standaert C, Fütterer JJ, Villeirs GM, Panebianco V, Walz J, *et al*. A systematic review on the role of imaging in early

recurrent prostate cancer. Eur Urol Oncol 2019;2:47-76.
25. Pietzsch HJ, Mamat C, Müller C, Schibli R. Single Photon Emission Computed Tomography Tracer. Recent Results Cancer Res 2020:216:227-82.
26. Cooperberg MR, Broering JM, Carroll PR. Risk assessment for prostate cancer metastasis and mortality at the time of diagnosis. J Natl Cancer Inst 2009;101:878-87.
27. Chaoying L, Chao M, Xiangrui Y, Yingjian H, Gang Z, Yunhan R, *et al*. Risk factors of bone metastasis in patients with newly diagnosed prostate cancer. Eur Rev Med Pharmacol Sci 2022;26:391-8.
28. Yamada Y, Naruse K, Nakamura K, Taki T, Tobiume M, Zennami K, *et al*. Investigation of risk factors for prostate cancer patients with bone metastasis based on clinical data. Exp Ther Med 2010;1:635-9.
29. Lu YJ, Duan WM. Establishment and validation of a novel predictive model to quantify the risk of bone metastasis in patients with prostate cancer. Transl Androl Urol 2021;10:310-25.
30. Lavery HJ, Droller MJ. Do Gleason patterns 3 and 4 prostate cancer represent separate disease states? J Urol 2012;188:1667-75.
31. Rodríguez-Antolín A, Gómez-Veiga F, Alvarez-Osorio JK, Carballido-Rodriguez J, Palou-Redorta J, Solsona-Narbón E, *et al.* Factors that predict the development of bone metastases due to prostate cancer: Recommendations for follow-up and therapeutic options. Actas Urol Esp 2014;38:263-9.
32. Hong H, Liang D, Liu Q, Wu G, Sun R, Liu J, *et al*. Value of transrectal contrast-enhanced ultrasound with clinical indicators in the prediction of bone metastasis in prostate cancer. Quant Imaging Med Surg 2022;12:1750-61.
33. Tucci M, Zichi C, Buttigliero C, Vignani F, Scagliotti GV, Di Maio M. Enzalutamide-resistant castration-resistant prostate cancer: Challenges and solutions. Onco Targets Ther 2018;11:7353-68.
34. Bray F, Laversanne M, Sung H, Ferlay J, Siegel RL, Soerjomataram I, *et al*. Global cancer statistics 2022: GLOBOCAN estimates of incidence and mortality worldwide for 36 cancers in 185 countries. CA Cancer J Clin 2024;74:229-63.
35. Karki R, Man SM, Kanneganti TD. Inflammasomes and cancer. Cancer Immunol Res 2017;5:94-9.
36. Diem S, Schmid S, Krapf M, Flatz L, Born D, Jochum W, *et al*. Neutrophil-to-lymphocyte ratio (NLR) and platelet-to-lymphocyte ratio (PLR) as prognostic markers in patients with non-small cell lung cancer (NSCLC) treated with nivolumab. Lung Cancer 2017;111:176-81.
37. Paget S. The distribution of secondary growths in cancer of the breast. Cancer Metastasis Rev 1889;8:98-101.
38. Bello JO, Olanipekun OO, Babata AL. Prognostic value of neutrophil-to-lymphocyte ratio in castration resistant prostate cancer: Single-centre study of Nigerian men. Niger J Clin Pract 2019;22:511-5.